Analytical Modeling of Multidirectional Entrainment in Three-Phase Gas-Liquid-Liquid Flows with Oilfield Applications in High Gas Rate Wellbores and Flowlines

Anand S. Nagoo

Nagoo & Associates LLC

6535 Valleyside Road, Austin, Texas 78731, United States of America

nagoo@nagoo-associates.com

Keywords: Analytical multiphase flow modeling, multidirectional entrainment, three-phase gas-liquid-liquid entrainment, annular-mist flow, wet-gas flow, mist flow

Abstract

In the high gas rate annular flows of wellbores and flowlines transporting multiphase petroleum fluids, the bi-directional entrainment of liquid-in-gas and gas-in-liquid significantly affects the pressure drops in these production systems. The changes to the mass flow rates and densities of the phases due to the varying entrained phase fractions necessarily alters the phase volume fractions, velocities and the different pressure gradients. When three phases of gas, oil and water are present, there is now quad-directional entrainment, with the gas-in-oil, gas-in-water, oil-in-gas and water-in-gas entrainments occurring simultaneously. This latter scenario is the norm in oilfield annular-dispersed droplet flows. This work introduces, for the first time, step-by-step calculations of a wholly-analytical development of these averaged multidirectional entrainment equations for use in the annular-to-mist flow modeling with various degrees of entrainment. Then, for the final validation aspect of the paper, both lab and actual oilfield datasets of annular-mist and mist flows from the published literature are selected to unambiguously demonstrate how the analytical equations of this work compare against these verifiable, cross-referable entrainment datasets. In terms of practical usage, this contribution establishes an analytical, physics-based, mist flow limit for the least possible pressure drop in a gas-liquid or gas-liquid-liquid closed-conduit flow – which can be used to screen faulty pressure gauge data downhole in a wellbore or on surface flowlines. This analytical limit can equivalently be used to screen physically-implausible multiphase hydrodynamic models.

Introduction

The interaction and behavior of a particle field and its carrier medium (or media) has long since been the subject of investigation in academic and industrial communities. Bibliographic surveys are abundant in special cases of this general subject and are usually application-specific, e.g., the prediction of water droplets in a heated nuclear fuel channel for nuclear reactor safety investigations (Leung, 1977; Reyes, Jr., 1986).

Annular-dispersed gas-liquid or gas-liquid-liquid flows are special cases of this general problem in which a liquid film with large numbers of small bubbles flows adjacent to the conduit wall and surrounds a central gas core laden with liquid droplets. This is alternatively referred to as annular gas-liquid or gas-liquid-liquid flow with multi-directional entrainment – with the direction of entrainment being either in one way, from the liquid to the gas core, or in multiple ways, between the gas and the adjacent flowing liquid (or liquids).

Crucial parameters in the above scenario are the fraction of the total liquid flow entrained as droplets or other (wispy) structures in the gas core and the fraction of total gas flow entrained as large numbers of small bubbles in the liquid film (or films). These parameters represent the net or integral effects of liquid droplet deposition and formation (sometimes called entrainment or atomization), and gas bubble entrainment. Several opinions as to the possible mechanisms responsible for these microphysical flow processes exist in the literature (e.g., Wallis, 1969; Hewitt, 1986; Oliemans et al., 1986; Azzopardi, 1997; Sawant et al., 2008). Reviews of various gas-liquid inter-phase entrainment modeling approaches are also abundant (e.g., Hewitt and Hall-Taylor, 1970; Brown, 1978; Martin, 1983; Govan, 1990; Han, 2005; Schubring, 2009).

Herein, we present new, simple-to-compute, step-by-step calculations of a wholly-analytical development describing averaged multi-directional inter-phase entrainment in the special case of annular-dispersed gas-liquid (bi-directional, two-phase entrainment) and gas-liquid-liquid flows (quad-directional, three-phase entrainment). In the detailed formulations below, the key insight gained with regards to this special category of multiphase flow with averaged inter-phase entrainment, is that only the mass fluxes and densities of phases in the flowing multiphase mixture need to be corrected to accurately account for inter-phase entrainment when used together with averaged multiphase hydrodynamic models (i.e., mass, momentum and energy balance equations). In this work, the multiphase hydrodynamic model used to generate results can be found in Nagoo (2013) and is given in computational form for practical use within the simulator described in Nagoo (2018a).

In general, therefore, a multiphase hydrodynamic model (sometimes called a "total pressure gradient model") will need to be corrected for its ability to reliably account for multidirectional entrainment by modifying the j-mass fluxes, G_j, and j-densities, ρ_j, of all j phases in the flowing multiphase mixture in accordance to their analytical closure equations given in this work, as depicted in the generic form below:

$$\overbrace{\left(\frac{\Delta P_{mix}}{\Delta L}\right)}^{\text{hydrodynamic}} = \overbrace{fn\left(inputs,\langle s_j\rangle,G_j^{corr},\rho_j^{corr}\right)}^{\text{friction}}$$
$$+\overbrace{fn\left(inputs,\langle s_j\rangle,\rho_j^{corr}\right)}^{\text{hydrostatic}} \quad (1)$$
$$-\overbrace{fn\left(inputs,\langle s_j\rangle,G_j^{corr},\rho_j^{corr}\right)}^{\text{convective acceleration (+ve) or deceleration (-ve)}}$$

In Eqn. 1, ‘inputs’ represent system parameters and other input data (e.g., inclination, diameter, wall roughness, etc.), and $\langle s_j\rangle$ is the phase-j averaged volume fraction. Also, for non-Newtonian annular gas-liquid or gas-liquid-liquid flows with multidirectional inter-phase entrainment, the non-Newtonian j-viscosity must incorporate corrected j-mass fluxes and j-densities in its definition when used in the frictional pressure gradient term of Eqn. 1.

In looking at the form and dependencies of Eqn. 1 above, it now becomes abundantly clear just how dominant the roles that averaged volume fractions and averaged entrainment fractions (included in the corrected mass fluxes and densities) play in relation to pressure calculation in averaged multiphase pipe flows. Of explanatory significance, is the simple and unique way these equations describe the competing effects of volume fraction, entrainment fraction and the frictional, hydrostatic and convective acceleration/deceleration pressure gradients. Indeed, with this new analytical understanding, it is now becomes obvious *why* prior total pressure gradient models performed so badly in the past in the special cases of annular gas-liquid and gas-liquid-liquid flows with multidirectional inter-phase entrainment – as clearly shown, all of the pressure gradients are very strongly affected by the corrections to the mass fluxes and densities.

In a controlled lab experiment without entrainment, all the terms on the right-hand side of Eqn. 1 above are expressed in terms of known system quantities and therefore it is evident that averaged volume fraction is the only unknown quantity to be measured (or modeled). Therefore, in the general case of multiphase flows without entrainment, the most important scientific implication is that it is now possible to falsify these models since uncertainties are now focused in one directly measurable variable – the averaged volume fraction. In the special case of multiphase flows with entrainment, falsification is still obtainable because averaged entrainment fraction can also be objectively measured in addition to averaged volume fraction.

Formulation and Discussion of the New Analytical Multidirectional Entrainment Equations

For the development of the analytical multidirectional entrainment equations below, we first start with the simpler case of two-phase liquid (phase 1) and gas (phase 2) annular flow with bi-directional entrainment.

Now, in general, for a phase-j flowing in a multiphase mixture of two or more phases, we can write:

$$\rho_j = \frac{G_j}{\langle u_j\rangle} = \frac{j\ mass\ flux}{j\ volume\ flux} \quad (2)$$

In this case, for phase 1 being entrained into phase 2, if we first look at j = 2, we can correct the above mass flux and volume flux for j = 2 to account for this as:

$$\rho_{2\leftarrow1}^{corr} = \frac{G_2 + G_{1\to2}^{entr}}{\langle u_2\rangle + \langle u_{1\to2}^{entr}\rangle} \quad (3)$$

Similarly, in general, entrainment is defined as:

$$E_{j\to k(\neq j)} = \frac{G_{j\to k(\neq j)}^{entr}}{G_j} \quad (4)$$

Therefore, in this case, for phase 1 being entrained into phase 2, if we look at j = 1, we can write Eqn. 4 as:

$$E_{1\to2} = \frac{G_{1\to2}^{entr}}{G_1} = \frac{\cancel{\rho_1}\langle u_{1\to2}^{entr}\rangle}{\cancel{\rho_1}\langle u_1\rangle} = \frac{\langle u_{1\to2}^{entr}\rangle}{\langle u_1\rangle} \quad (5)$$

Putting Eqns. (2), (4) and (5) in (3), we get:

$$\rho_{2\leftarrow1}^{corr} = \frac{\rho_2\langle u_2\rangle + \rho_1\langle u_1\rangle E_{1\to2}}{\langle u_2\rangle + \langle u_1\rangle E_{1\to2}} \quad (6)$$

Next, in general, by definition:

$$G_j^{corr} = G_j - G_{j\to k(\neq j)}^{entr} \quad (7)$$

Now, the principal insight with regards to bi-directional two-phase entrainment is that during the entrainment of phase 1 into phase 2, simultaneously, the corrected phase 2 (which we will call phase 2′) will itself be entraining into the continuously diminishing phase 1 (i.e., the corrected phase 1 which we will call phase 1′). For phase 1 being entrained into phase 2, if we look at j = 1, we can thus write:

$$G_1^{corr} = G_1 - G_{1\to2}^{entr}$$
$$\Rightarrow \cancel{\rho_{1'\leftarrow2'}^{corr}}\langle u_1^{corr}\rangle = \cancel{\rho_{1'\leftarrow2'}^{corr}}\langle u_1\rangle - \cancel{\rho_{1'\leftarrow2'}^{corr}}\langle u_{1\to2}^{entr}\rangle \quad (8)$$

Then, putting Eqn. (5) in (8), we get:

$$\langle u_1^{corr}\rangle = \langle u_1\rangle\left(1-E_{1\to2}\right) \quad (9)$$

If we now look at j = 1′, we can now re-state Eqn. 3 as:

$$\rho_{1'\leftarrow 2'}^{corr} = \frac{G_1^{corr} + G_{2'\rightarrow 1'}^{entr}}{\langle u_1^{corr}\rangle + \langle u_{2'\rightarrow 1'}^{entr}\rangle} \tag{10}$$

And similar to Eqn. 5, for phase 2′ being entrained into phase 1′, if we look at j = 2′, we can re-write Eqn. 4 as:

$$E_{2'\rightarrow 1'} = \frac{G_{2'\rightarrow 1'}^{entr}}{G_{2'}} = \frac{\cancel{\rho_{2\leftarrow 1}^{corr}}\langle u_{2'\rightarrow 1'}^{entr}\rangle}{\cancel{\rho_{2\leftarrow 1}^{corr}}\langle u_2\rangle} = \frac{\langle u_{2'\rightarrow 1'}^{entr}\rangle}{\langle u_2\rangle} \tag{11}$$

Then, putting Eqns. (2), (4), (8), (9) and (11) in (10), we can write:

$$\rho_{1'\leftarrow 2'}^{corr} = \frac{\rho_1\langle u_1\rangle(1-E_{1\rightarrow 2}) + \rho_{2\leftarrow 1}^{corr}\langle u_2\rangle E_{2'\rightarrow 1'}}{\langle u_1\rangle(1-E_{1\rightarrow 2}) + \langle u_2\rangle E_{2'\rightarrow 1'}} \tag{12}$$

Next, similar to Eqn. 8, for phase 2′ being entrained into phase 1′, if we look at j = 2′, we can write:

$$G_{2'}^{corr} = G_{2'} - G_{2'\rightarrow 1'}^{entr}$$
$$\Rightarrow \cancel{\rho_{2\leftarrow 1}^{corr}}\langle u_{2'}^{corr}\rangle = \cancel{\rho_{2\leftarrow 1}^{corr}}\langle u_2\rangle - \cancel{\rho_{2\leftarrow 1}^{corr}}\langle u_{2'\rightarrow 1'}^{entr}\rangle \tag{13}$$

And, putting Eqn. (11) in (13), we get:

$$\langle u_{2'}^{corr}\rangle = \langle u_2\rangle(1-E_{2'\rightarrow 1'}) \tag{14}$$

Thus, from the quite simple development above, if bi-directional entrainment is occurring between any two arbitrary phase 1 (heavier phase) and phase 2 (lighter phase), then the phase densities and mass fluxes change and need to be corrected, in order of step-by-step calculation, as follows:

$$\boxed{\begin{array}{lll} Step\ 1\ (Eqn.\ 6): & \rho_2 & \rightarrow \rho_{2\leftarrow 1}^{corr} \\ Step\ 2\ (Eqn.\ 12): & \rho_1 & \rightarrow \rho_{1'\leftarrow 2'}^{corr} \\ Step\ 3\ (Eqn.\ 14): & G_2 & \rightarrow G_{2'}^{corr} \\ Step\ 4\ (Eqn.\ 9): & G_1 & \rightarrow G_1^{corr} \end{array}} \tag{15}$$

Now, a post-analysis of any of the relations above will reveal both a physically sensible and internal self-consistency. Testing the limits of Eqns. (6) and (9):

I. For Eqn. 6, $\left.\rho_{2\leftarrow 1}^{corr}\right|_{at\ E_{1\rightarrow 2}=0} = \rho_2$

II. Also, for Eqn. 6,

$$\left.\rho_{2\leftarrow 1}^{corr}\right|_{at\ E_{1\rightarrow 2}=1} = \overbrace{\left(\frac{G_{mix}}{\langle u_{mix}\rangle}\right)}^{\substack{homogenous\ mixture\ density \\ (mist\ flow)}}$$

III. For Eqn. 9, $\left.G_1^{corr}\right|_{at\ E_{1\rightarrow 2}=0} = G_1$

IV. Also, for Eqn. 9, $\left.G_1^{corr}\right|_{at\ E_{1\rightarrow 2}=1} = \overbrace{0}^{mist\ flow}$

Now, before we can similarly begin to test the limits of Eqns. (12) and (14), we note that the relationship between $E_{1\rightarrow 2}$ and $E_{2'\rightarrow 1'}$ can be stated analytically. To demonstrate this, we first know that if $E_{1\rightarrow 2}=0$ (i.e. no entrainment of phase 1 into phase 2), then $\rho_{1'\leftarrow 2'}^{corr}$ in Eqn. 12 must be $=\rho_1$. Clearly, the only value of $E_{2'\rightarrow 1'}$ that satisfies this fact is 0. Therefore, we know the functional form of $E_{2'\rightarrow 1'}$ in relation to $E_{1\rightarrow 2}$ must, at a minimum, be expressed as:

$$E_{2'\rightarrow 1'} = E_{1\rightarrow 2} \times\ ? \tag{16}$$

Next, from a relative volume flux standpoint, if $E_{1\rightarrow 2}=1$ (i.e. full entrainment of phase 1 into phase 2), then $\langle u_{2'}^{corr}\rangle$ must be $=\langle u_2\rangle - \langle u_1\rangle$. Using Eqn. 9, this relative volume flux can be re-arranged as:

$$\left.\langle u_{2'}^{corr}\rangle\right|_{at\ E_{1\rightarrow 2}=1} = \langle u_2\rangle\left(1-\frac{\langle u_1\rangle}{\langle u_2\rangle}\right) \tag{17}$$

Now, comparing Eqn. (17) with (14), we see that a general relationship for $E_{2'\rightarrow 1'}$ that will satisfy both of the limits depicted in Eqns. (16) and (17) is:

$$E_{2'\rightarrow 1'} = E_{1\rightarrow 2}\left(\frac{\rho_2}{\rho_1}\frac{G_1}{G_2}\right)^{p-(p-1)E_{1\rightarrow 2}} \tag{18}$$

In Eqn. 18 above, the parameter, p, can be any non-negative integer number and still satisfy the limits in Eqns. (16) and (17) at $E_{1\rightarrow 2}=1$. We are thus faced with a positive-infinite number of possibilities for a functional form of $E_{2'\rightarrow 1'}$, even though it is clear how this variable must behave in the limits of $E_{1\rightarrow 2}=0$ and $E_{1\rightarrow 2}=1$. We therefore must make a hypothesis. We postulate based on the physical argument, that $E_{2'\to 1'}$ should be related to $E_{1\to 2}$ such that the entrainment of the less dense phase, phase 2′, into the more dense phase, phase 1′, will more easily occur when there is a lower amount of phase 1′ to entrain into (i.e., at higher values of $E_{1\to 2}$). This idea is *only* honored for p values of 2 and greater in Eqn. 18. With no logical reason for choosing any value of p greater than 2, we must therefore set p at its simplest valid value according to our hypothesis, i.e. at p = 2. So, our revised form for Eqn. 18 is:

$$E_{2'\to 1'} = E_{1\to 2}\left(\frac{\rho_2}{\rho_1}\frac{G_1}{G_2}\right)^{2-E_{1\to 2}} \qquad (19)$$

With an analytical relation now in hand for $E_{2'\to 1'}$, we can now go back to testing the limits of Eqns. (12) and (14). We see that:

I. For Eqn. 12,

$$\rho^{corr}_{1'\leftarrow 2'}\Big|_{at\ E_{1\to 2}=0\ and\ E_{2'\to 1'}=0} = \rho_1$$

II. Also, for Eqn. 12,

$$\rho^{corr}_{1'\leftarrow 2'}\Big|_{at\ E_{1\to 2}=1} = \overbrace{\left(\frac{G_{mix}}{\langle u_{mix}\rangle}\right)}^{\substack{homogenous\\ mixture\\ density\\ (mist\ flow)}}$$

III. For Eqn. 14,

$$G^{corr}_{2'}\Big|_{at\ E_{1\to 2}=0\ and\ E_{2'\to 1'}=0} = G_2$$

IV. Also, for Eqn. 14,

$$G^{corr}_{2'}\Big|_{at\ E_{1\to 2}=1} = \overbrace{\left(\frac{G_{mix}}{\langle u_{mix}\rangle}\right)}^{\substack{homogenous\\ mixture\\ density\\ (mist\ flow)}}\cdot\left(\langle u_2\rangle - \langle u_1\rangle\right)$$

As before, we see that there is a clear mathematical self-consistency to all of the analytical equations developed so far.

The next question that arises is the physical maximum possible limit on the derived relation $E_{2'\to 1'}$ in Eqn. 19 above. Aside from the fact that its analytical and functional form honors all mathematical consistency checks, if unrestricted, this form of $E_{2'\to 1'}$ can yield values greater than 1. Additionally, it is a common scenario in field-scale applications where the mass flux of phases changes according to the changing pressure and temperature flowing conditions, for example, as with complex petroleum fluids in petroleum industry annular-mist flows. Hence, at the point that the mass flux of phase 1 attains the same value as the mass flux of phase 2, then it is reasonable to assume that it will be unlikely that any further entrainment of phase 2 into phase 1 will occur. So from Eqn. 19, the physical maximum value of $E_{2'\to 1'}$ is ρ_2/ρ_1, where all of phase 1 is entrained into phase 2, and the mass flux of phase 1 is equal to that of phase 2. If we consider the case where phase 1 is a liquid and phase 2 is a gas, for example, then this would mean that at any given entrainment fraction of the liquid in the gas, the entrainment fraction of the gas in the liquid (either in the liquid film or in the liquid droplets or in the liquid wisps, or all of the previous) can at most be equal to $E_{liquid\to gas}\left(\rho_{gas}/\rho_{liquid}\right)^{2-E_{liquid\to gas}}$.

Therefore, the final, corrected form of Eqn. 19 is:

$$E_{2'\to 1'} = \min\left(\begin{array}{l} E_{1\to 2}\left(\frac{\rho_2}{\rho_1}\frac{G_1}{G_2}\right)^{2-E_{1\to 2}}, \\ E_{1\to 2}\left(\frac{\rho_2}{\rho_1}\right)^{2-E_{1\to 2}} \end{array}\right) \qquad (20)$$

From Eqn. 20, it can be inferred that entrainment behavior would be quite different between systems with a high density contrast (e.g. laboratory experiments) versus systems with a lower density contrast (e.g. field systems). This is quite important by itself and is unrelated to any conduit size scaling issue when going from lab-scale to field-scale. As seen from Eqn. 20, a higher density contrast places limits on how much of phase 2 can be entrained into phase 1, especially at higher phase 1 rates relative to phase 2. Conversely, a lower density contrast permits higher phase 2 entrainment into phase 1. These analytically developed descriptions mesh quite well with physical observations both in the lab and field.

Next, it should be noted that at full entrainment of phase 1 into phase 2, homogenous mixture (mist flow) equations are fully recovered according to the development above and this results in wholly-analytical relationships between phase 2 volume fraction, $\langle s_2\rangle$, $E_{1\to 2}$ and $E_{2'\to 1'}$ for a two-phase system.

Additionally, it is shown that for a two-phase system with bi-directional entrainment occurring, the only additional unknown aside from $\langle s_2\rangle$ in Eqn. 1, is $E_{1\to 2}$. $E_{1\to 2}$ can, of course, be either provided (measured) or predicted using any preferred reliable correlation (e.g., Ishii and Mishima, 1982). In the special scenario of fully entrained mist flow, both $\langle s_2\rangle$ and $E_{1\to 2}$ have values of unity and Eqn. 1 therefore achieve its highest prediction performance possible (because it becomes wholly analytical) for this special scenario. We will clearly demonstrate this fact in comparing this mist flow limit of the bi-directional entrainment equations developed in this section with observed (cross-referable, published) two-phase mist flow applications both in the lab and the field in the next section.

Continuing the generalized, analytical development above, it is now easy to extend our insights for bi-directional two-phase entrainment to a third arbitrary phase, phase 3 (lightest phase). For phases 1 and 2 being entrained into phase 3 (and vice-versa), if we look at j = 3, we can correct the mass flux and volume flux for j = 3 to account for this as:

$$\rho^{corr}_{3\overset{\leftarrow 1}{\leftarrow 2}} = \frac{G_3 + G^{entr}_{1\to 3} + G^{entr}_{2\to 3}}{\langle u_3\rangle + \langle u^{entr}_{1\to 3}\rangle + \langle u^{entr}_{2\to 3}\rangle} \tag{21}$$

For phase 1 being entrained into phase 3, if we look at j = 1, we can write Eqn. 4 as:

$$E_{1\to 3} = \frac{G^{entr}_{1\to 3}}{G_1} = \frac{\cancel{\rho_1}\langle u^{entr}_{1\to 3}\rangle}{\cancel{\rho_1}\langle u_1\rangle} = \frac{\langle u^{entr}_{1\to 3}\rangle}{\langle u_1\rangle} \tag{22}$$

Similarly, for phase 2 being entrained into phase 3, if we look at j = 2, we can write Eqn. 4 as:

$$E_{2\to 3} = \frac{G^{entr}_{2\to 3}}{G_2} = \frac{\cancel{\rho_2}\langle u^{entr}_{2\to 3}\rangle}{\cancel{\rho_2}\langle u_2\rangle} = \frac{\langle u^{entr}_{2\to 3}\rangle}{\langle u_2\rangle} \tag{23}$$

Putting Eqns. (4), (22) and (23) in (21), we get:

$$\rho^{corr}_{3\overset{\leftarrow 1}{\leftarrow 2}} = \frac{\rho_3\langle u_3\rangle + \rho_1\langle u_1\rangle E_{1\to 3} + \rho_2\langle u_2\rangle E_{2\to 3}}{\langle u_3\rangle + \langle u_1\rangle E_{1\to 3} + \langle u_2\rangle E_{2\to 3}} \tag{24}$$

Now, the critical insight with regards to quad-directional three-phase entrainment is that during the entrainment of phases 1 and 2 into phase 3, simultaneously, the corrected phase 3 (which we will call phase 3′) will itself be entraining into the continuously diminishing phases 1 and 2 (i.e., the corrected phases 1 and 2 which we will call phases 1′ and 2′, respectively). For phase 1 being entrained into phase 3, if we look at j = 1, we can write:

$$\begin{gathered} G^{corr}_1 = G_1 - G^{entr}_{1\to 3} \\ \Rightarrow \cancel{\rho^{corr}_{1'\leftarrow 3'}}\langle u^{corr}_1\rangle = \cancel{\rho^{corr}_{1'\leftarrow 3'}}\langle u_1\rangle - \cancel{\rho^{corr}_{1'\leftarrow 3'}}\langle u^{entr}_{1\to 3}\rangle \end{gathered} \tag{25}$$

Putting Eqn. (22) in (25), we get:

$$\langle u^{corr}_1\rangle = \langle u_1\rangle\left(1 - E_{1\to 3}\right) \tag{26}$$

Similarly, for phase 2 being entrained into phase 3, if we look at j = 2, we can write:

$$\begin{gathered} G^{corr}_2 = G_2 - G^{entr}_{2\to 3} \\ \Rightarrow \cancel{\rho^{corr}_{2'\leftarrow 3'}}\langle u^{corr}_2\rangle = \cancel{\rho^{corr}_{2'\leftarrow 3'}}\langle u_2\rangle - \cancel{\rho^{corr}_{2'\leftarrow 3'}}\langle u^{entr}_{2\to 3}\rangle \end{gathered} \tag{27}$$

Putting Eqn. (23) in (27), we get:

$$\langle u^{corr}_2\rangle = \langle u_2\rangle\left(1 - E_{2\to 3}\right) \tag{28}$$

If we now look at j = 1′, we can now re-state Eqn. 2 as:

$$\rho^{corr}_{1'\leftarrow 3'} = \frac{G^{corr}_1 + G^{entr}_{3'\to 1'}}{\langle u^{corr}_1\rangle + \langle u^{entr}_{3'\to 1'}\rangle} \tag{29}$$

Similar to Eqn. 22, for phase 3′ being entrained into phase 1′, if we look at j = 3′, we can write Eqn. 4 as:

$$E_{3'\to 1'} = \frac{G^{entr}_{3'\to 1'}}{G_{3'}} = \frac{\cancel{\rho^{corr}_{3\overset{\leftarrow 1}{\leftarrow 2}}}\langle u^{entr}_{3'\to 1'}\rangle}{\cancel{\rho^{corr}_{3\overset{\leftarrow 1}{\leftarrow 2}}}\langle u_3\rangle} = \frac{\langle u^{entr}_{3'\to 1'}\rangle}{\langle u_3\rangle} \tag{30}$$

And, putting Eqns. (25), (26) and (30) in (29), we can write:

$$\rho^{corr}_{1'\leftarrow 3'} = \frac{\rho_1\langle u_1\rangle\left(1 - E_{1\to 3}\right) + \rho^{corr}_{3\overset{\leftarrow 1}{\leftarrow 2}}\langle u_3\rangle E_{3'\to 1'}}{\langle u_1\rangle\left(1 - E_{1\to 3}\right) + \langle u_3\rangle E_{3'\to 1'}} \tag{31}$$

We can now repeat the analysis above for phase 2′. If we look at j = 2′, we can write:

$$\rho^{corr}_{2'\leftarrow 3'} = \frac{G^{corr}_2 + G^{entr}_{3'\to 2'}}{\langle u^{corr}_2\rangle + \langle u^{entr}_{3'\to 2'}\rangle} \tag{32}$$

Similar to Eqn. 23, for phase 3′ being entrained into phase 2′, if we look at j = 3′, we can write Eqn. 4 as:

$$E_{3'\to 2'} = \frac{G^{entr}_{3'\to 2'}}{G_{3'}} = \frac{\cancel{\rho^{corr}_{3\overset{\leftarrow 1}{\leftarrow 2}}}\langle u^{entr}_{3'\to 2'}\rangle}{\cancel{\rho^{corr}_{3\overset{\leftarrow 1}{\leftarrow 2}}}\langle u_3\rangle} = \frac{\langle u^{entr}_{3'\to 2'}\rangle}{\langle u_3\rangle} \tag{33}$$

And, putting Eqns. (27), (28) and (33) in (32), we can write:

$$\rho^{corr}_{2'\leftarrow 3'} = \frac{\rho_2\langle u_2\rangle\left(1 - E_{2\to 3}\right) + \rho^{corr}_{3\overset{\leftarrow 1}{\leftarrow 2}}\langle u_3\rangle E_{3'\to 2'}}{\langle u_2\rangle\left(1 - E_{2\to 3}\right) + \langle u_3\rangle E_{3'\to 2'}} \tag{34}$$

Lastly, for phase 3′ being entrained into phases 1′ and 2′, if we look at j = 3′, we can write:

$$G_{3'}^{corr} = G_{3'} - G_{3'\to 1'}^{entr} - G_{3'\to 2'}^{entr}$$
$$\Rightarrow$$
$$\cancel{\rho_{3\substack{\leftarrow 1\\ \leftarrow 2}}^{corr}}\left\langle u_{3'}^{corr}\right\rangle = \cancel{\rho_{3\substack{\leftarrow 1\\ \leftarrow 2}}^{corr}}\left\langle u_{3}\right\rangle - \cancel{\rho_{3\substack{\leftarrow 1\\ \leftarrow 2}}^{corr}}\left\langle u_{3'\to 1'}^{entr}\right\rangle - \cancel{\rho_{3\substack{\leftarrow 1\\ \leftarrow 2}}^{corr}}\left\langle u_{3'\to 2'}^{entr}\right\rangle \qquad (35)$$

And, putting Eqns. (30), (33) in (35), we get:

$$\left\langle u_{3'}^{corr}\right\rangle = \left\langle u_{3}\right\rangle\left(1 - E_{3'\to 1'} - E_{3'\to 2'}\right) \qquad (36)$$

Thus, from extended (yet still simple) development above, if quad-directional entrainment is occurring among any three arbitrary phase 1 (heaviest), phase 2 (lighter) and phase 3 (lightest) with entrainment between the three phases except between phases 1 and 2, then the phase densities and mass fluxes change and need to be corrected (in order of step-by-step calculation) as follows:

$$\boxed{\begin{array}{lcl} Step\ 1\ (Eqn.\ 24): \ \rho_3 & \to & \rho_{3\substack{\leftarrow 1\\ \leftarrow 2}}^{corr} \\ Step\ 2\ (Eqn.\ 34): \ \rho_2 & \to & \rho_{2'\leftarrow 3'}^{corr} \\ Step\ 3\ (Eqn.\ 31): \ \rho_1 & \to & \rho_{1'\leftarrow 3'}^{corr} \\ Step\ 4\ (Eqn.\ 36): \ G_3 & \to & G_{3'}^{corr} \\ Step\ 5\ (Eqn.\ 28): \ G_2 & \to & G_{2}^{corr} \\ Step\ 6\ (Eqn.\ 26): \ G_1 & \to & G_{1}^{corr} \end{array}} \qquad (37)$$

As in the previous bi-directional entrainment analysis, a similar post-analysis of any of the relations above will reveal both a physically sensible and internal, mathematical self-consistency. Testing the limits of Eqns. (24), (26) and (28), we see that:

I. For Eqn. 24,

$$\left.\rho_{3\substack{\leftarrow 1\\ \leftarrow 2}}^{corr}\right|_{\substack{at\ E_{1\to 2}=0\\ and\ E_{2\to 3}=0}} = \rho_3$$

II. Also, for Eqn. 24,

$$\left.\rho_{3\substack{\leftarrow 1\\ \leftarrow 2}}^{corr}\right|_{\substack{at\ E_{1\to 2}=1\\ and\ E_{2\to 3}=1}} = \overbrace{\left(\frac{G_{mix}}{\left\langle u_{mix}\right\rangle}\right)}^{\substack{homogenous\\ mixture\\ density\ (mist\ flow)}}$$

III. For Eqn. 26,

$$\left.G_1^{corr}\right|_{at\ E_{1\to 3}=0} = G_1$$

IV. Also, for Eqn. 26,

$$\left.G_1^{corr}\right|_{at\ E_{1\to 3}=1} = \overbrace{0}^{phase\ 1\ fully\ entrained}$$

V. For Eqn. 28,

$$\left.G_2^{corr}\right|_{at\ E_{2\to 3}=0} = G_2$$

VI. Also, for Eqn. 28,

$$\left.G_2^{corr}\right|_{at\ E_{2\to 3}=1} = \overbrace{0}^{phase\ 2\ fully\ entrained}$$

Now, we note that the relationship between $E_{1\to 3}$ and $E_{3'\to 1'}$ can be stated analytically using the same line of reasoning as in the preceding bi-directional entrainment development. In this case, an analogous relation to Eqn. 20 is:

$$E_{3'\to 1'} = \min\left(\begin{array}{c} E_{1\to 3}\left(\dfrac{\rho_3}{\rho_1}\dfrac{G_1}{G_3}\right)^{2-E_{1\to 3}}, \\ E_{1\to 3}\left(\dfrac{\rho_3}{\rho_1}\right)^{2-E_{1\to 3}} \end{array}\right) \qquad (38)$$

And similarly, for phase 3′ entrainment into phase 2′, we can write the analogous relationship between $E_{2\to 3}$ and $E_{3'\to 2'}$ as:

$$E_{3'\to 2'} = \min\left(\begin{array}{c} E_{2\to 3}\left(\dfrac{\rho_3}{\rho_2}\dfrac{G_2}{G_3}\right)^{2-E_{2\to 3}}, \\ E_{2\to 3}\left(\dfrac{\rho_3}{\rho_2}\right)^{2-E_{2\to 3}} \end{array}\right) \qquad (39)$$

So, with analytical relations now in place for both $E_{3'\to 1'}$ and $E_{3'\to 2'}$, we can now return to testing the limits of Eqns. (31), (34) and (36). We see from Eqn. 37, that:

I. For Eqn. 31,

$$\left.\rho_{1'\leftarrow 3'}^{corr}\right|_{at\ E_{1\to 3}=0\ and\ E_{3'\to 1'}=0} = \rho_1$$

II. Also, for Eqn. 31,

$$\left.\rho_{1'\leftarrow 3'}^{corr}\right|_{\substack{at\ E_{1\to 3}=1\\ and\ E_{2\to 3}=1}} = \overbrace{\left(\frac{G_{mix}}{\left\langle u_{mix}\right\rangle}\right)}^{\substack{homogenous\ mixture\\ density\ (mist\ flow)}}$$

III. For Eqn. 34,

$$\rho^{corr}_{2'\leftarrow 3'}\Big|_{at\ E_{2\to3}=0\ and\ E_{3'\to2'}=0} = \rho_2$$

IV. Also, for Eqn. 34,

$$\rho^{corr}_{2'\leftarrow 3'}\Big|_{\substack{at\ E_{2\to3}=1\\ and\ E_{1\to3}=1}} = \overbrace{\left(\frac{G_{mix}}{\langle u_{mix}\rangle}\right)}^{\substack{homogenous\ mixture\\ density\ (mist\ flow)}}$$

V. For Eqn. 36,

$$G^{corr}_{3'}\Big|_{\substack{at\ E_{1\to3}=0\ and\ E_{3'\to1'}=0\\ at\ E_{2\to3}=0\ and\ E_{3'\to2'}=0}} = G_3$$

VI. Also, for Eqn. 36,

$$G^{corr}_{3'}\Big|_{\substack{at\ E_{1\to3}=1\\ and\ E_{2\to3}=1}} = \overbrace{\left(\frac{G_{mix}}{\langle u_{mix}\rangle}\right)}^{\substack{homogenous\ mixture\\ density\ (mist\ flow)}} \cdot\left(\langle u_3\rangle - \langle u_1\rangle - \langle u_2\rangle\right)$$

Summarily, we see that there is a clear mathematical self-consistency to all the equations developed in this section. It should also be noted that at full entrainment of phases 1 and 2 into phase 3, three-phase mist flow equations are fully recovered according to the development above and this results in wholly-analytical relationships between phase 3 volume fraction, $\langle s_3\rangle$, $E_{1\to3}$, $E_{2\to3}$, $E_{3'\to1'}$ and $E_{3'\to2'}$ for a three-phase system.

Additionally, it is shown that for a three-phase system with quad-directional entrainment occurring between phase 3 and the other phases, the only additional unknowns aside from $\langle s_3\rangle$ and $\langle s_2\rangle$ in Eqn. 1 are $E_{1\to3}$ and $E_{2\to3}$. Both $E_{1\to3}$ and $E_{2\to3}$ can be either provided (measured) or predicted using a preferred correlation (e.g., Ishii and Mishima, 1982). In the special scenario of fully entrained mist flow, $\langle s_3\rangle$, $E_{1\to3}$ and $E_{2\to3}$ have values of unity and Eqn. 1 thus achieve its highest prediction performance possible (because it becomes wholly analytical) for this special scenario. We will demonstrate this fact when we compare this limit of the quad-directional entrainment equations developed in this section with the three-phase mist flow field dataset below.

Unbiased Validation of the New Analytical Multidirectional Entrainment Equations

For unbiased validation of the analytical multidirectional entrainment equations developed in the previous section, we select a few high-quality lab and field datasets from the published (cross-referable) literature that is readily accessible. These validation comparisons provide a gist of the extent and high degree of reliability of the analytical multidirectional entrainment equations of this work when compared against independently-verifiable lab observations and field data.

An important note on the calculations shown in this section are that the corrected mass fluxes and densities of Eqns. (15) and (37) – the main results of this paper – are first used to calculate the phase volume fractions and then these corrected phase volume fractions are used in the calculation of the total pressure gradient.

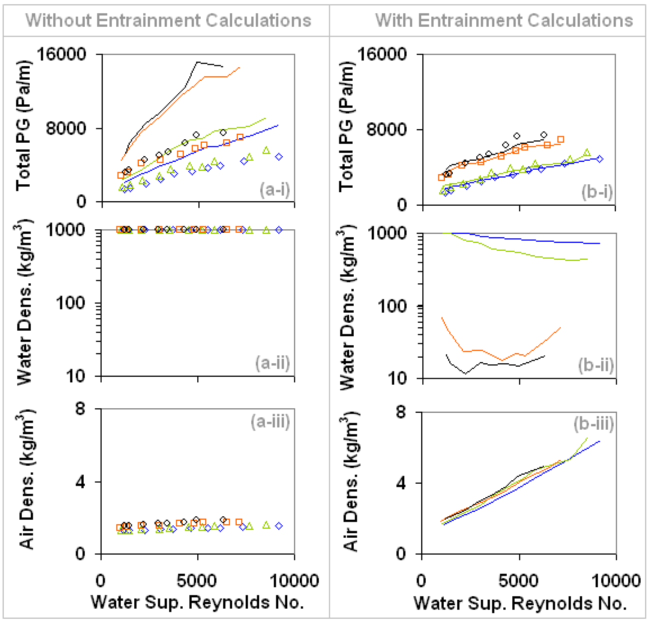

Figure 1: Demonstrating the validity of the analytical equations in this work against the vertical annular flow dataset of Hewitt et al. (1961). Liquid entrainment fraction is predicted with the Ishii and Mishima (1982) correlation. Lines are calculations and points are measurements. The blue diamonds, green triangles, orange squares and black circles correspond to air superficial Reynolds numbers of 114661, 132175, 205703 and 224584, respectively.

Fig. 1 above shows a classic vertical upward annular flow dataset of Hewitt et al. (1961) in which both the averaged phase volume fractions and total pressure gradients were measured. Fig. 1(a-i) shows how far off the total pressure gradient ("Total PG" above) can be when compared with measurements if entrainment is not accounted for. Figs. 1(a-ii) shows the water densities that are used in the calculations if not accounting for entrainment and Fig. 1(a-iii) shows the air densities that are used in calculations if not accounting for entrainment.

If we now account for bi-directional entrainment by using the Ishii and Mishima (1982) model predictions for water entrainment in air, in concert with the analytical entrainment corrections in Eqn. 15, then we see in Fig. 1(b-i) that our calculations for total pressure gradient are quite accurate. Indeed, Fig. 1(b-ii) shows how the water densities (and thus water superficial velocities) are reduced as a result of the bi-directional entrainment occurring and Fig. 1(b-iii) shows how the air densities (and thus air superficial velocities) are increased as well. Notice from these results we see that the higher the liquid entrainment, the lower the water density and the higher the air density. This comparison against the carefully controlled lab dataset shown represents a clear validation of the analytical entrainment equations presented in the previous section as well as the *need* for properly accounting for multi-directional entrainment.

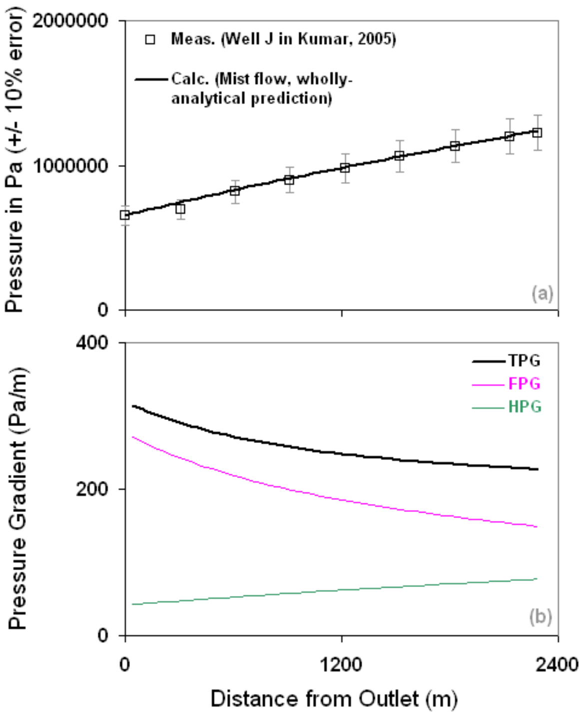

Figure 2: Analytical prediction of the flowing pressure survey of a BP North America two-phase gas-water vertical well (well "J" of Kumar, 2005) with the mist flow model.

Next, we look at a vertical well field dataset of oilfield water and natural gas at high pressure and temperature – this is well "J" of Kumar (2005), which is one of the North America producing wells of the BP company. The stated water production rate for this well is 2 barrels per day with a high gas-to-water ratio (GWR) of 345,000 standard cubic feet per barrel. For this well, flowing pressure survey data was available for comparison against the mist flow calculations of this work. As seen in Fig. 2(a) above, the fully entrained mist flow calculations compare quite favorably with the field data. Also, as seen in Fig. 2(b), the frictional pressure gradient (FPG) dominates the hydrostatic pressure gradient (HPG) in the total pressure gradient (TPG) profile along the well, which is a defining characteristic of annular-mist and fully entrained mist flows.

Last, we simulate the outlet pressure (given the inlet pressure) of the 73 miles, 36-inch internal diameter gas-condensate water flow line as reported in Crowley et al. (1986). As seen in Fig. 3, the outlet pressure is predicted accurately with the multi-directional analytical mist flow model and using a horizontal flow line approximation.

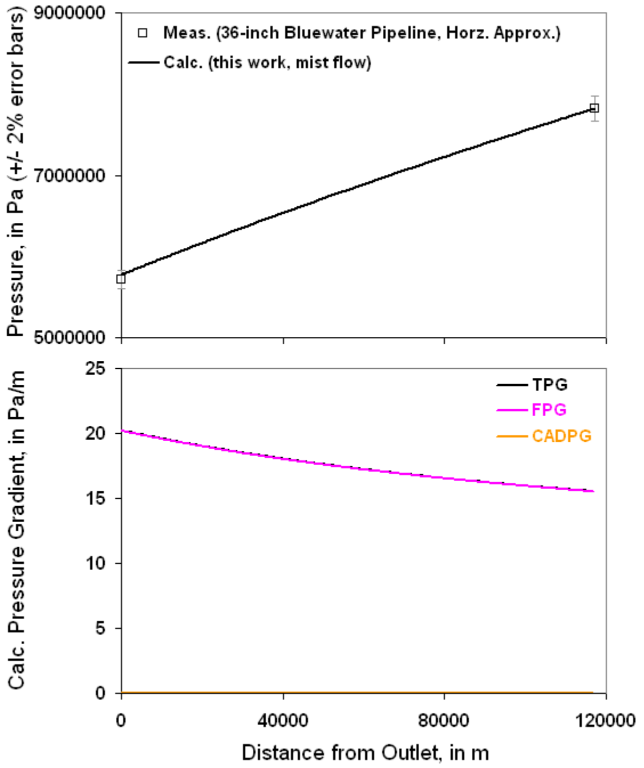

Figure 3: Analytical prediction of the outlet pressure of the 73 miles, 36-inch diameter Bluewater three-phase gas-condensate-water flowline in Crowley et al. (1986) using the mist flow model.

Conclusions

This work introduces, for the first time, step-by-step calculations of a wholly-analytical development of the averaged multidirectional entrainment equations for use in the annular-mist to full mist flow modeling with various degrees of entrainment. Such a development not only provides simple-to-compute and reliably predictable analytical equations for use in multiphase computational codes, but more importantly, provides deeper insight into the multi-directional entrainment process itself. It is now clear, for example, *why* multiphase flow meters in the wet gas regime will require liquid mass flux and density adjustments for improving their accuracy. It is also clear *why* prior averaged total pressure gradient models in the literature predicted annular-to-mist flows so poorly in the past regardless of their degree of complexity without making the appropriate corrections for mass fluxes and phase densities.

In terms of practical usage, this contribution establishes a physics-based, analytical mist flow limit for the least possible pressure drop in a gas-liquid or gas-liquid-liquid closed-conduit flow – which can be used to screen faulty pressure gauge data downhole in a wellbore or on surface flowlines. For example, in using wellbore lift curves (described in Nagoo, 2018b), a simultaneous calculation of a mist flow limit should be performed for screening downhole oil and gas well pressure gauge data. This analytical limit can equivalently be used to screen physically-implausible multiphase hydrodynamic models.

Finally, both lab and actual oilfield datasets of annular-mist and mist flows from the published literature are selected to demonstrate how the analytical equations of this work compare against these verifiable, cross-referable entrainment datasets. Of course, much more independent datasets can be predicted as desired using the presented analytical entrainment equations using the step-by-step formulation described in Eqns. (15) and (37) – the main results of this work.

References

Leung, J. C. M.: Occurrence of critical heat flux during blowdown with flow reversal, ANL Report 77-4, Jan (1977)

Reyes, Jr., J. N.: A study of non-equilibrium dispersed two-phase flow, Ph.D. Dissertation, U. of Maryland (1986)

Wallis, G. B. One-dimensional two-phase flow. McGraw-Hill, (1969)

Hewitt, G. F.: Co-current and counter-current two phase annular flow, 9th Australasian Fluid Mech. Conf., Auckland, December 8-12 (1986)

Oliemans, R. V. A., Pots, B. F. M., Trompe, N.: Modelling of annular dispersed two-phase flow in vertical pipes, Intl. J. of Multiphase Flow, v. 12, no. 5, pp. 711-732 (1986)

Azzopardi, B. J.: Drops in annular two-phase flow, Intl. J. Multiphase Flow, v. 23, Suppl., pp. 1-53 (1997)

Sawant, P., Ishii. M., Mori, M.: Droplet entrainment correlation in vertical upward co-current annular two-phase flow, Nucl. Eng. Des., v. 238, pp. 1342-1352 (2008)

Hewitt, G. F., Hall-Taylor, N. S.: Annular two-phase flow, Permagon Press (1970)

Brown, D. J.: Disequilibrium in annular flow, Ph.D. Thesis, Oxford U. (1978)

Martin, C. J.: Annular two-phase flow, Ph.D. Dissertation, Oxford U. (1983)

Govan, A. H.: Modelling of vertical annular and dispersed two-phase flows, Ph.D. Thesis, Imperial College (1990)

Han, H.: A study of entrainment in two-phase upward cocurrent annular flow in a vertical tube, Ph.D. Thesis, Dept. of Mechanical Eng., U. of Saskatchewan (2005)

Schubring, D.: Behavior interrelationships in annular flow, Ph.D. Thesis, U. of Wisconsin-Madison (2009)

Nagoo, A. S.: Pipe Fractional Flow Theory – Principles and Applications, http://hdl.handle.net/2152/65197, Ph.D. Dissertation, The University of Texas at Austin, Dec. (2013)

Nagoo, A. S.: Multiphase AP Engine – an analytical multiphase flow simulator, www.nagoo-associates.com (2018a)

Ishii, M., Mishima, K.: Liquid transfer and entrainment correlation for droplet-annular flow, 7th Intl. Heat Transfer Conf., Munchen (1982)

Hewitt, G. F., King, I., Lovegrove, P. C.: Holdup and pressure drop measurements in the two-phase annular flow of air-water mixtures, UK AERE Report R3764, June (1961)

Kumar, N.: Improvements for flow correlations for gas wells experiencing liquid loading, Society of Petroleum Engineers, SPE-92049 (2005)

Crowley, C. J., Sam, R. G., Rothe, P. H.: Investigation of two-phase flow in horizontal and inclined pipes at large pipe size and high gas density, Project PR-172-507, Pipeline Research Committee, AGA, February (1986)

Nagoo, A. S.: Gas Velocity-Based Lift Curves for Quantifying Lost Liquids Production in Oil-Rich Permian and Delaware Basin Horizontal Gas Wells, SPE-191772, Society of Petroleum Engineers Liquids-Rich Basins Conference - North America, Midland, Texas, U.S.A., Sep. (2018b)